

# INTEGRATING REMOTE SENSING, GIS AND HYDROLOGIC MODELS FOR PREDICTING LAND COVER CHANGE IMPACTS ON SURFACE RUNOFF AND SEDIMENT YIELD IN A CRITICAL WATERSHED IN MINDANAO, PHILIPPINES

J. R. Santillan<sup>a,\*</sup>, M. M. Makinano<sup>b</sup>, E. C. Paringit<sup>a</sup>

<sup>a</sup> Research Laboratory for Applied Geodesy & Space Technology, Training Center for Applied Geodesy & Photogrammetry, University of the Philippines (UP) Diliman, Quezon City 1101, Philippines - jrsantillan@up.edu.ph

<sup>b</sup> College of Engineering & Information Technology, Caraga State University (CSU), Butuan City 8600, Philippines

**KEY WORDS:** Land Cover, Hydrology, Integration, Modelling

## ABSTRACT:

This paper presents an integrated approach involving Remote Sensing (RS), Geographic Information System (GIS) and hydrologic models to characterize and quantify the impacts of land cover change in tropical watersheds, specifically in the critical Taguibo Watershed in Mindanao, Philippines. A rainfall-runoff model based on the US Soil Conservation Service-Curve Number (SCS-CN) and a sediment yield model based on the Modified Universal Soil Loss Equation (MUSLE) were constructed to estimate the impacts of land cover change on the volume of runoff and sediment yield during rainfall events. Landsat ETM+ and MSS images were analyzed to obtain land cover maps needed for model parameterizations. The applicability of the integrated RS-GIS-hydrologic modeling approach for the prediction of land cover change impacts was tested using three scenarios of land cover change. The ability of the framework to quantifiably predict the potential hydrologic implications of land cover change offers watershed planners and decision-makers a valuable tool for evaluating the affectivity of proposed land cover rehabilitation strategies in minimizing runoff and sediment yield during rainfall events in watershed ecosystems.

## 1. INTRODUCTION

The negative impacts of land cover change to the natural environment especially in watershed ecosystems have been a widely recognized problem throughout the world. Forest cover reduction through deforestation and conversion for agricultural purposes can alter a watershed's response to rainfall events, that often leads to increased volumes of surface runoff and greatly increase the incidence of flooding and sedimentation of receiving water bodies (McColl and Aggett, 2007). The detection of these changes is crucial to provide information as to what and where the changes have occurred and to analyze the impacts of these changes.

In the Philippines, the Taguibo Watershed in Northeastern Mindanao (Figure 1) exemplifies the case of severe impacts of land cover change to watershed runoff and sediment yield. This watershed has experienced extensive alteration of its land cover due to the presence of several logging industries with Timber License Agreements (TLAs) in the 1960's until the early 1980s (DENR, 2003). Its forest cover was severely reduced by logging and clear-felling, and the former logged-over areas were opened up to intensive farming, thereby accommodating the influx of farmers who were intent in cultivating semi-temperature high value vegetables. These historical changes in the watershed's land cover and the continuous illegal logging activities have led to a very serious condition of the watershed. Significant increase in runoff volume during rainfall events and extensive sedimentation of rivers and streams due to severe soil erosion in the watershed's landscape have taken place (DENR, 2003). As the surface water of Taguibo Watershed is the main source for domestic and agricultural needs of the people living nearby, the alarming situations have prompted the Department

of Environment and Natural Resources (DENR) to come up with rehabilitation efforts such as reforestation of formerly logged areas and agro-forestation in highly eroded landscapes to mitigate the problem of increased runoff generation and high rate of sedimentation. While these efforts to address the negative impacts of land cover change are necessary, they can only be fruitful if information on the location and extent of the areas that need rehabilitation is available. Moreover, relevant information that portrays space-time relationships of land cover to hydrological functions is often required to properly formulate and evaluate mitigation measures and rehabilitation strategies.

Remote Sensing (RS) has played a major role in watershed research and hydrological sciences (Engman, 1995). Land cover information derived from RS images has been used in a variety of hydrological modeling studies, most especially in surface runoff predictions and sediment yield estimations (e.g., Sekhar and Rao, 2002). The addition of Geographic Information System (GIS) technology further enhanced these capabilities and added confidence in the accuracy of modelled watershed conditions, improved the efficiency of the modeling process and increased the estimation capability of hydrologic models (Bhuyan et al., 2003).

While several studies have utilized RS and GIS with hydrologic modeling for assessing the impacts of land cover change to the hydrologic response of watersheds to rainfall events, a majority of them is focused on modeling the watershed's response to future changes in land cover (e.g., McColl and Aggett, 2007). Few studies relate the hydrological responses of watershed to its past and present conditions. In watershed management, this is of paramount importance as the information derived from modeling can be directly related to the changes in land cover as

---

\* Corresponding author.

well as to the overall condition of the modelled watershed. Proper mitigation measures and efficient conservation strategies can then be formulated upon examination of the root causes of watershed problems, and hence, leading to its rehabilitation.

In this paper, an integrated approach using RS, GIS and hydrologic modeling is presented to detect and analyze the past and present land cover conditions of a watershed and to estimate the impacts of the detected changes on surface runoff and sediment yield. The integrated approach is also used to approximate the success or failure of planned rehabilitation measures and strategies in addressing land cover induced hydrological problems in watersheds, especially in the study area.

## 2. METHODS

### 2.1 Characteristics of the study area

The Taguibo Watershed has a drainage area of 75.532 km<sup>2</sup>. It is composed of plains, steep hills and mountains. According to the Taguibo River Watershed Management Plan (DENR, 2003), majority of the soils in the watershed belongs to hydrologic soil group B (loamy and silty-loamy soils) which indicates medium runoff potential (SCS, 1985). Clayey and shallow soils belonging to hydrologic soil group D (high runoff potential) are generally observed in areas with 50% or more slope. The study area has no distinct dry season; pronounced rainfall occurs from November to January.

### 2.2 Landsat image analysis and change detection

Orthorectified Landsat MSS and ETM+ images covering the study area acquired on April 17, 1976 (path 120, row 54) and May 22, 2001 (path 112, row 54), with pixel resolution of 57-m and 28.5-m, respectively, were obtained from the Global Land cover Facility (GLCF), University of Maryland (<http://glcf.umd.edu>). These images are part of the GLCF GeoCover collection which consists of decadal Landsat data which has been orthorectified and processed to a higher quality standard. Documentations on the orthorectification process can be found in the GLCF GeoCover website at <http://glcf.umd.edu/research/portal/geocover/>.

The images were radiometrically corrected to at-sensor radiance using the standard Landsat calibration formulas and constants. A fast atmospheric correction using dark-object subtraction was also implemented. Normalised Difference Vegetation Index (NDVI) images were also computed from the radiometrically and atmospherically-corrected images. Only the portions of the images covering the study area were subjected to image analysis. Six (6) land cover classes were identified from the images through visual interpretations with the aid of existing land cover and topographic maps published by the DENR as references. These include barren areas, built-up areas, forest, grassland, mixed vegetation (combination of forest, tree plantation, shrub land and grassland) and water bodies. Built-up areas were only detected on the 2001 Landsat ETM+ image. We assumed that built-up areas in the 1976, although present, were limited in extent so that they were not visible in the Landsat MSS images primarily because of the sensor's low

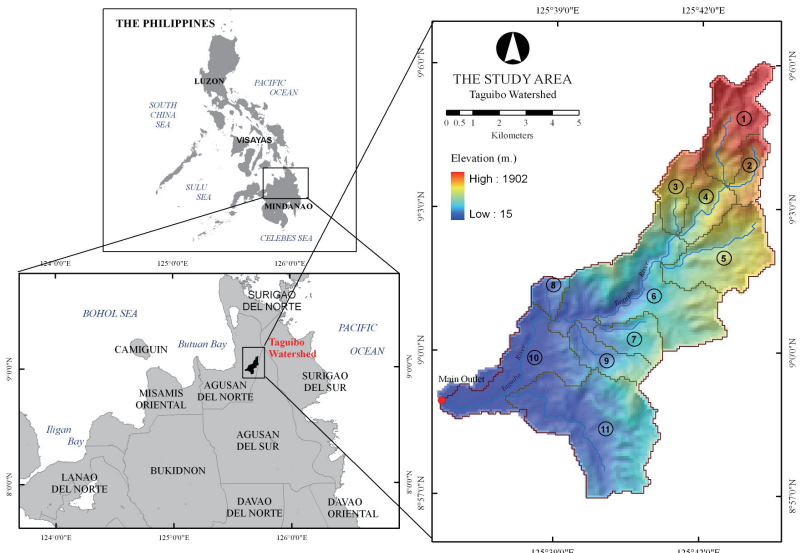


Figure 1. The Taguibo Watershed in Mindanao Island, Philippines.

spatial resolution. Representative samples of each class were collected from the images for supervised image classification. The training samples were collected in such a way that the assumption of normal distribution of the Maximum Likelihood Classifier (MLC) is satisfied and that the separability of the classes (computed using the Jeffries-Matusita Distance) is  $\geq 1.7$ . Another independent set of samples were likewise collected for accuracy assessment. The MLC was used to classify the Landsat images (all bands) with the inclusion of the NDVI. The accuracy of each classified images were independently assessed. Initial trials were done to classify the input images using the Minimum Distance, Mahalanobis Distance and Parallelepiped classifiers. However, the accuracies of each classified image using these classifiers were significantly lower ( $<90\%$ ) than those of the MLC-classified images. The two resulting land cover maps were then subjected to post-classification comparison change detection analysis to examine the location, extent and distribution of land cover change in the study area. The 2001 land cover map was first re-sampled to 57-m resolution prior to change detection.

### 2.3 Rainfall-runoff modelling

Rainfall-runoff modeling was performed using the Soil Conservation Service-Curve Number (SCS-CN) model (SCS, 1985). The SCS-CN model is a well established method in hydrologic engineering and environmental impact analyses and has been very popular because of its convenience, simplicity, authoritative origins, and its responsiveness to four readily grasped watershed properties: soil type, land use/land cover and treatment, surface condition, and antecedent moisture condition (Ponce and Hawkins, 1996). The popular form of the SCS-CN model is:

$$Q = \frac{(P - I_a)^2}{P - I_a + S} \text{ for } I_a \leq P, \text{ otherwise } Q = 0 \quad (1)$$

$$I_a = \lambda S \text{ where } S = \frac{25400}{CN} - 254. \quad (2)$$

$P$  is total rainfall,  $I_a$  is initial abstraction,  $Q$  is direct runoff,  $S$  is potential maximum retention which can range  $(0, \infty)$ , and  $\lambda$  is initial abstraction coefficient or ratio. All variables are in millimeters (mm) except for  $\lambda$  which is unitless. The initial abstraction  $I_a$  includes short-term losses due to evaporation, interception, surface detention, and infiltration and its ratio to  $S$

describes  $\lambda$  which depends on climatic conditions and can range  $(0, \infty)$ . The SCS has adopted a standard value of 0.2 for  $\lambda$  (SCS, 1985) but this can be estimated through calibration with field measured discharge data. The potential maximum retention  $S$  characterizes the watershed's potential for abstracting and retaining storm moisture, and therefore, its direct runoff potential (Ponce and Hawkins, 1996).  $S$  is directly related to land cover and soil infiltration through the parameter  $CN$  or "curve number", a non-dimensional quantity varying in the range (0–100) and depends on the antecedent moisture condition of the watershed. Higher  $CN$  values indicate high runoff potential. For normal antecedent moisture conditions (AMCII, 5-day antecedent rainfall (AR) is 0.5 – 1.1 inches), the curve number values for land cover types and soil textures (hydrologic soil groups B and D) prevalent in the study area were obtained from SCS (1985). The AMCII  $CN$  values can be converted to AMCI (dry condition,  $AR < 0.5$  inches) and AMCIII (wet condition,  $AR > 1.1$  inches) using the formula of Chow, et al. (1988).

The SCS-CN model was implemented using the Hydrologic Engineering Center-Hydrological Modeling System or HEC-HMS (USACE, 2000). The SCS-CN model was co-implemented with the Clark Unit Hydrograph method (for sub-watershed routing of runoff), the Exponential Baseflow Recession model, and the Muskingum-Cunge model for channel routing. A thorough discussion of these three additional models can be found in Chow et al. (1988). Model parameterizations were done using HEC-GeoHMS (USACE, 2003), the ArcView GIS-based pre-processor of HEC-HMS. HEC-GeoHMS was used to delineate 11 sub-watershed boundaries. Average values of  $CN$  values for each sub-watershed were computed based on the 2001 and 1976 land cover maps. Initial parameter values for the Baseflow Recession, Clark Unit Hydrograph, and Muskingum-Cunge models were derived from a combination of HEC-GeoHMS processing algorithms with data inputs from river profile and cross-section surveys conducted in April 2007.

The HEC-HMS model was calibrated using rainfall events recorded at the inner portion of the watershed, and discharge hydrographs measured at the main outlet for the June 25-27, 2007 period. Records of 5-day accumulated rainfall depths before the simulation showed an  $AR > 1.1$  inches, indicating AMCIII. Model calibration was done to fine-tune the  $\lambda$  parameter of the SCS-CN model, and the time-related parameters of the baseflow recession model and Clark Unit Hydrograph model, which were initially assumed. The absence of sources of land cover information for the state of the watershed when the calibration data were collected prompted us to parameterize the model using the 2001 land cover map. During this period, available satellite images were all covered with clouds. We assumed that no significant change in land cover had occurred from 2001-2007. The Nash-Sutcliffe (1970) Coefficient of Model Efficiency,  $E$ , was used to evaluate the performance of the hydrologic model during calibration.  $E$  ranges between  $-\infty$  and 1.0 (1 included) with  $E = 1$  being the optimal value. Values between 0.0 and 1.0 are generally viewed as accepted levels of performance while values  $\leq 0.0$  indicates that the mean observed value is a better predictor than the simulated value, which indicates unacceptable model performance.

#### 2.4 Sediment yield modelling

A sediment yield model capable of representing the impacts of land cover and their associated changes in time and space to

sediment yield was constructed using the Modified Universal Soil Loss equation (MUSLE) of Williams (1975), an event-based, empirical soil erosion model. The MUSLE is formulated as:  $S_y = R' \cdot K \cdot L \cdot S \cdot C \cdot P$  where  $R' = a(Q \cdot q_p)^b$ .  $S_y$  is the sediment yield in metric tons for the specific rainfall event,  $R'$  is the runoff erosivity factor,  $Q$  is the volume of runoff in  $m^3$  produced by the event,  $q_p$  is the peak flow rate in  $m^3 s^{-1}$  and  $a$  and  $b$  are location-dependent coefficients that can be estimated through calibration with measured sediment yield. The terms  $K$ ,  $L$ ,  $S$ ,  $C$  and  $P$  are the standard MUSLE factors which represent soil erodibility, slope length, slope steepness, cover management and support practices, respectively. Among the five factors, the  $C$  factor is the most important in sediment yield estimations if changes in land cover are to be accounted. The  $C$  factor estimates the effect of ground cover conditions, soil conditions, and general management practices on erosion rates. This is where the land cover information derived from RS image analysis is integrated for the estimation of sediment yield.  $C$  factor values for the different land cover classes in the study area were obtained from the studies of Jain et al. (2005).

A sediment transport model based on the sediment routing equations of the Soil and Water Assessment Tool (SWAT) model (Neitsch et al., 2005) was used to route the computed sediment concentrations at the sub-watershed outlet through the channels until the main outlet of the watershed is reached. The sediment transport capacity of a channel segment during the time step is determined by  $T(t) = xV(t)^y$ , where  $T(t)$  is the maximum concentration of sediment that can be transported by water (metric tons/ $m^3$ );  $V(t)$  is the instantaneous flow velocity (m/s) during the time step,  $t$ ;  $x$  is a user-defined calibration coefficient, and  $y$  is a user-defined exponent which normally varies from 1-2. Bed deposition occurs when the computed sediment concentration is greater than  $T(t)$ .

The sediment yield model, implemented in a spreadsheet application, was loosely coupled with the SCS-CN-based rainfall-runoff model in order to derive  $Q$  and  $q_p$  needed to compute for  $S_y$ . The mean MUSLE factor values for each sub-watershed were computed from the soil map, SRTM DEM and the year 2001 land cover map using available algorithms in HEC-GeoHMS. The sediment yield model was calibrated with the hourly measured sediment yield collected at the main outlet of the study area from 12:00PM of June 26 to 10:00AM of June 27, 2007 at 1-hour interval. Optimization of the values of  $a$  and  $b$  in the MUSLE equation and the values of  $x$  and  $y$  in the sediment transport capacity equation was done so that the simulated sediment yield conforms to the observed data.  $E$  was likewise used to evaluate the performance of the model during calibration.

#### 2.5 Runoff and sediment yield predictions in three land cover conditions

The calibrated rainfall-runoff and sediment yield models were then used to compute  $Q$  and  $S_y$  in the 11 sub-watersheds under three land cover conditions namely, 2001, 1976 and a "rehabilitated" condition. The latter was derived from the analysis of the 2001 image, where areas in urgent need of rehabilitation were identified. This includes areas classified as grassland and barren. In the "rehabilitated" land cover map, grassland areas were re-classified as "forest" while barren areas were converted to "agro-forested areas" which is composed of mixed vegetation. This is in accordance to the rehabilitation strategy planned by the DENR.

In using the calibrated hydrologic models for predicting the impacts of land cover change, only the *CN* parameter of the SCS-CN model and the *C* factor of the MUSLE model were altered as these parameters have direct relationship with land cover. The same rainfall events used previously for model calibration were utilized again in the simulations. The results of the simulations were then analyzed (1) to determine the runoff and sediment yield responses of the watershed in 3 land cover conditions, (2) to identify how different are these responses from each other, and (3) to verify if rehabilitation strategies could help in the reduction of runoff and sediment yield in the watershed under the assumption that the same rainfall events will take place.

### 3. RESULTS AND DISCUSSION

#### 3.1 Land cover change in the Taguibo Watershed

The land cover maps of the study area for 1976 and 2001 derived from Maximum Likelihood-classified Landsat images are shown in Figure 2 (a and b). The 1976 land cover map has an overall classification accuracy of 96.06% and kappa statistic of 0.95 while the 2001 land cover map obtained 96.79% accuracy and kappa statistic of 0.96. Producer's and User's Accuracies of each land cover type were greater than 90% in both maps.

Figure 2c shows the "rehabilitated" land cover map of the watershed. In this map, the watershed is in a condition where barren areas and grasslands detected from the 2001 Landsat ETM+ image as consequences of anthropogenic disturbances, were rehabilitated through their conversion to mixed vegetation and reforestation, respectively.

The changes in land cover from 1976-2001 with respect to the total area of the watershed are presented in Table 1. The analysis showed a 6.52% reduction in forest cover, a 13.69% reduction in mixed vegetation, a 4.46% increase in barren areas and 15.54% increase in grassland in the study area in the span of 25 years. The 4.46% increase in barren areas maybe attributed to more recent human-induced alterations of the watershed such as increase in agricultural areas, forest denudation due to illegal logging and slash-and-burn farming and harvesting of planted trees (DENR, 2003). A portion of the 6.52% reduction in forest cover maybe also due to these mentioned activities. On the other hand, the reduction in mixed vegetation cover and increased in grassland areas may be the result of the historical modification of the watershed landscape by logging industries and the influx of farmers who were intent to cultivate the logged-over areas by planting high-valued vegetables and rice crops. When the potential for agricultural productivity of these areas have lessened through time, these were left over for grasses to grow (DENR, 2003). A very good basis of this is the 15.54% increase in grassland areas. The

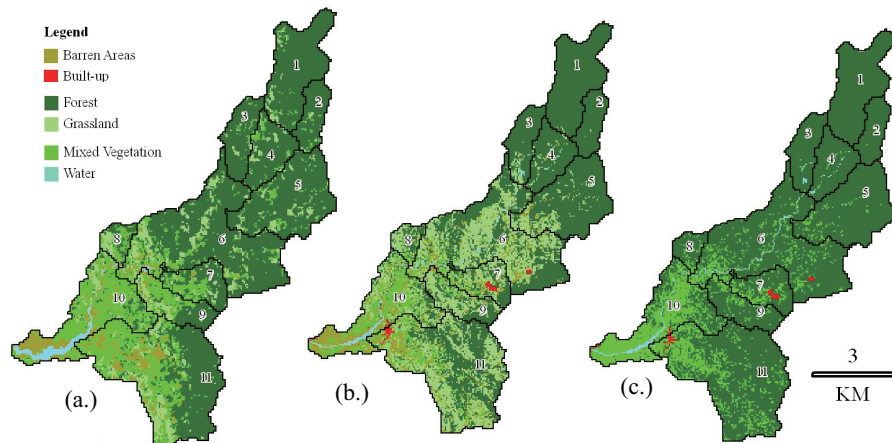


Figure 2. Land cover maps of the Taguibo Watershed derived from the analysis of Landsat images: (a.) 1976, (b.) 2001 and (c.) rehabilitated. Numbers indicate sub-watersheds.

effect of these land cover changes on the watershed's surface runoff and sediment yield are discussed in the next sections.

Table 1. 1976-2001 land cover change statistics.

Land cover classes	1976 Area (km <sup>2</sup> )	2001 Area (km <sup>2</sup> )	% Change from 1976 with respect to total watershed area
Barren areas	5.201	8.569	+4.46
Built-up areas	-	0.300	+0.40
Forest	46.287	41.366	-6.52
Grassland	7.271	19.008	+15.54
Mixed Vegetation	15.703	5.359	-13.69
Water	1.070	0.930	-0.19

#### 3.2 Calibrated rainfall-runoff and sediment yield models

Figure 3 shows the results of the calibration of the rainfall-runoff model with field measured discharge data for the June 25-27, 2007 period. The computed *E* value is 0.92 indicating a highly acceptable performance. However, there are portions of the simulated hydrograph that overestimate the outflow and underestimate the peak discharge. The average residual was computed as 2.95 m<sup>3</sup>/s. Plausible explanations for these slight differences in the simulated and measured hydrographs are the fact that the land cover information used to parameterise during model calibration may be different to the actual land cover of the study area when the field data were collected.

Figure 4 shows the results of the calibration of the sediment yield model. Although the model performed satisfactorily (*E*=0.62), the peak of the simulated sediment yield was not able to match the observed peak. The average residual was computed at 5.22 metric tons. One of the possible reasons for this is the underestimation of peak discharge by the calibrated rainfall-runoff model where values of *Q* and *q<sub>p</sub>* were obtained and used to compute *S<sub>p</sub>*.

Nevertheless, as the computed *E* values of the models are above satisfactory, the models could be used with modest accuracy for runoff predictions and sediment yield estimations under different land cover conditions of the study area.

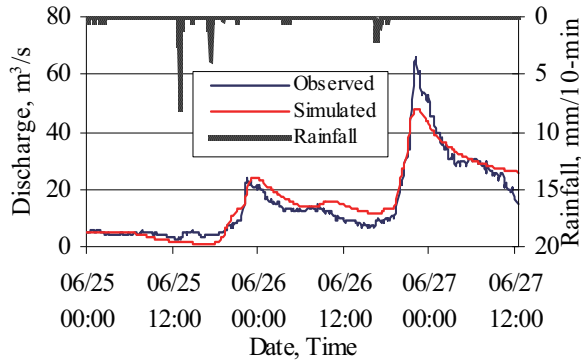


Figure 3. Rainfall-runoff model calibration

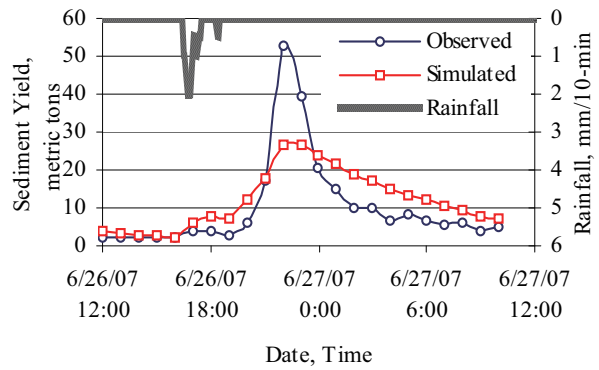


Figure 4. Sediment yield model calibration result.

**3.3 Runoff and sediment yield estimates for the 3 land cover conditions**

Model predicted accumulated runoff volume and sediment yield at each outlet of the 11 sub-watersheds are shown in Figures 5 and 6. It can be observed that there were minimal differences in the accumulated runoff volumes and sediment yield in sub-watersheds 1, 2, 3 and 4 for the three land cover conditions. This could be due to minimal changes in land cover in these sub-watersheds. The graph in Figure 5 also illustrated the high runoff potential of these particular sub-watersheds. Although the majority of land cover in these areas is forest, the runoff generated during rainfall events is high. This demonstrates the effects of steep slopes in these areas that give minimal span for the rainwater to infiltrate the ground.

Pronounced variation in runoff volumes and sediment yield in the 1976 and 2001 land cover conditions were observed for the remaining watersheds, most especially in sub-watersheds 5, 6, 7, 9, 10 and 11. It can be stated that changes in major land cover types in these areas, specifically the increase of barren areas and grasslands and the decrease in forest and mixed vegetation covers (Table 2) have directly affected the hydrologic response of the watershed to rainfall events – rainfall interception and infiltration have been affected such that huge volumes of surface runoff are generated and more soils are being eroded and transported to the sub-watershed outlets. Sub-watershed 11 was found to have the highest sediment yield among the 11 sub-watersheds which could be due to intensive agricultural activities in this area (DENR, 2003).

In terms of total surface runoff accumulated at the main outlet of the watershed (Table 3), model predictions showed that accumulated runoff volume in 1976 were 10.62% lesser than in 2001. In terms of accumulated sediment yield (Table 4), model predictions showed that sediment yield of the study area in 1976 is 37.31% lesser than in 2001. Rehabilitation of the sub-watersheds through planting of mixed vegetation and reforestation was found to be effective. It was computed that rehabilitation could reduce the accumulated runoff volume and sediment yield in 2001 by 23.85% and 95.95%, respectively. These results provide quantitative estimations that rehabilitation strategies proposed by the DENR, should they be 100% implemented, are most likely to reduce the volume of runoff and sediment yield generated during rainfall events in the Taguibo Watershed.

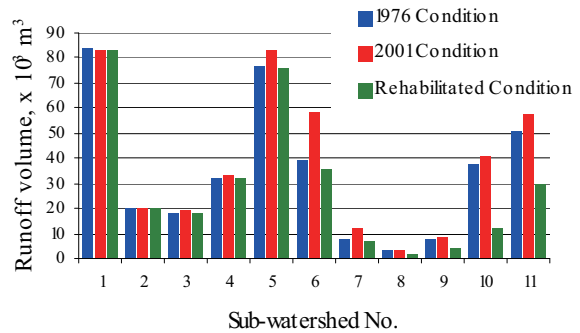


Figure 5. Model predicted runoff volume (accumulated) for the 11 sub-watersheds from June 25-27, 2007 under 3 land cover conditions.

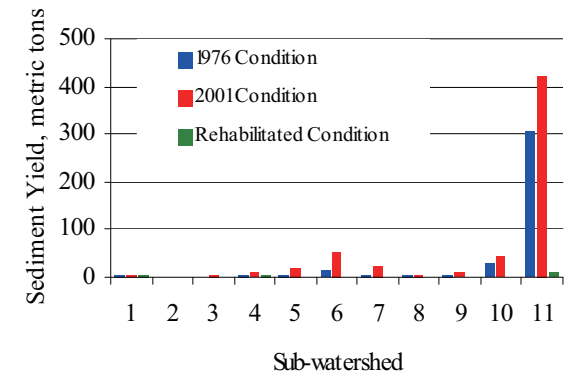


Figure 6. Model predicted sediment yield for the 11 sub-watersheds from June 25-27, 2007 under 3 land cover conditions.

Table 2. Major land cover change from 1976-2001 in sub-watersheds (SW) 5, 6, 7, 9, 10 and 11. Percentage of change is computed with respect to the area of the sub-watershed.

SW No.	Area, km <sup>2</sup>	% change in Barren Areas	% change in Forest	% change in Grassland	% change in Mixed Vegetation
5	8.748	+3.80	-3.68	+5.91	-6.20
6	16.483	+7.27	-26.95	+27.05	-8.96
7	3.224	+12.52	-18.22	+25.93	-23.51
9	3.459	+2.71	+1.91	+24.05	-27.82
10	9.056	+9.01	+3.35%	+13.64	-21.12
11	16.540	+2.39	-5.66%	+23.84	-21.20



Table 3. Accumulated runoff volumes in 3 land cover conditions (total for 11 sub-watersheds) for the June 25-27, 2007 period.

Land cover condition	Accumulated watershed runoff volume, $\times 10^3 \text{ m}^3$	% Difference from the 2001 condition
1976	376.771	- 10.62%
2001	421.540	
Rehabilitated	320.996	-23.85%

Table 4. Sediment yield in 3 land cover conditions (total for 11 sub-watersheds) for the June 25-27, 2007 period.

Land cover condition	Accumulated sediment yield, metric tons	% Difference from the 2001 condition
1976	372.89	-37.31%
2001	594.86	
Rehabilitated	24.06	-95.95%

#### 4. CONCLUSIONS

We have presented an integrated RS-GIS-hydrologic modelling approach in predicting the impacts of land cover change in runoff and sediment yield in the critical Taguibo Watershed in Mindanao, Philippines. We expanded our analysis by incorporating the detected changes in land cover to the parameterization of rainfall-runoff and sediment yield models in a GIS environment. This allowed us to better understand the impacts of the land cover change to the increase in surface runoff and sediment yield during rainfall events in the Taguibo Watershed. The Landsat image analysis also provided us a very quick identification of areas that need rehabilitation. Using the hydrologic models, we tested planned rehabilitation strategies that were aimed to reduce surface runoff and sediment yield, and we were able to express the effectiveness of these strategies. Although the methods used in this study was applied in a relatively small watershed, its applicability to large watersheds and river basins is also possible as long as there are available RS images to derive land cover information needed for detecting and locating the changes, and for hydrologic modeling. With the availability over the internet of Landsat images acquired since 1972, the methods employed in this study can be readily applied for watershed land cover change monitoring, management and rehabilitation.

While the study has presented a systematic approach for rainfall-runoff and sediment yield model constructions through an RS-GIS-hydrologic modeling framework, only field measured data can assess the accuracy of the model predictions. Nevertheless, the ability of the framework to quantifiably predict the potential hydrologic implications of land cover change offers watershed planners and decision-makers a valuable tool for evaluating the affectivity of proposed land cover rehabilitation strategies in minimizing runoff and sediment yield during rainfall events in watershed ecosystems.

#### REFERENCES

Bhuyan, S.J., Koelliker, J.K., Marzen, L.J. and Harrington Jr., J.A., 2003. An integrated approach for water quality assessment of a Kansas watershed. *Environmental Modelling and Software*, 18, pp. 473-484.

Chow, V.T., Maidment, D.R. and Mays, L.W., 1988. *Applied Hydrology*. McGraw-Hill: New York, USA.

DENR, 2003. *Taguibo River Watershed Management Plan*. Department of Environment and Natural Resources, Caraga Region XIII, Butuan City, Agusan del Norte, Philippines.

Engman, E.T., 1995. The use of remote sensing data in watershed research. *Journal of Soil and Water Conservation*, 50(5), pp. 438-440.

Jain, M.K., Kothyari, U.C. and Ranga-Raju, K.G., 2005. GIS-based distributed model for soil erosion and rate of sediment outflow from catchments. *Journal of Hydraulic Engineering*, 131(9), pp. 755-769.

McColl, C. and Aggett, G., 2007. Land use forecasting and hydrologic model integration for improved land-use decision support. *Journal of Environment Management*, 84(4), pp. 494-512.

Neitsch, S.L., Arnold, J.G., Kiniry, J.R. and Williams, J.R., 2005. *Soil and Water Assessment Tool Theoretical Documentation Version 2005*. Grassland, Soil and Water Research Laboratory, Agricultural Research Service, and Blackland Research Center, Texas Agricultural Experiment Station, Temple, Texas, USA, 476pp.

Nash, J., and Sutcliffe, J., 1970. River flow forecasting through conceptual models, I - A discussion of principles. *Journal of Hydrology*, 10, pp. 282-290.

Ponce, V.M. and Hawkins, R.H., 1996. Runoff curve number: has it reached maturity? *Journal of Hydrologic Engineering*, 1, pp. 11-19.

SCS, 1985. *National Engineering Handbook, Section 4: Hydrology*. Soil Conservation Service, US Department of Agriculture, Washington D.C.

Sekhar, K.R. and Rao, B.V., 2002. Evaluation of sediment yield by using remote sensing and GIS: a case study from the Phulang Vagu watershed, Nizamaba District (A.P). *International Journal of Remote Sensing*, 23(20), pp. 4449-4509.

USACE, 2000. *Hydrologic Modeling System HEC-HMS Technical Reference Manual*. United States Army Corps of Engineers-Hydrologic Engineering Center: Davis, California.

USACE, 2003. *Geospatial Hydrologic Modelling Extension HEC-GeoHMS User's Manual, Version 1.1*. United States Army Corps of Engineers-Hydrologic Engineering Center: Davis, California.

Williams, J.R., 1975. Sediment routing for agricultural watersheds. *Water Resources Bulletin*, 11, 965-974.

#### ACKNOWLEDGEMENTS

The authors would like to thank the Philippine Council for Advanced Science and Technology Research and Development of the Department of Science and Technology (PCASTRD-DOST) for funding this work, and the University of the Philippines-Diliman for the Research Dissemination Grant and Travel Assistance provided to the first author that made possible the presentation of this paper in the 2010 ISPRS TCVIII Symposium.